



**SKRIPSI – ME 141501**

**PENGARUH PROFIL DAUN PROPELLER DAN INTERVAL TIP  
ROTOR TERHADAP EFISIENSI ROTOR PADA *MICRO QUAD-  
ROTOR* PADA KONDISI MELAYANG**

Georgius Suhud  
NRP. 4212 100 114

Dosen Pembimbing :  
Sutopo Purwono Fitri, S.T., M.Eng., Ph.D.  
Mizue Munekata, Ph.D.

**JURUSAN TEKNIK SISTEM PERKAPALAN**  
Fakultas Teknologi Kelautan  
Institut Teknologi Sepuluh Nopember  
Surabaya, Indonesia  
2016



**SKRIPSI – ME 141501**

**PENGARUH PROFIL DAUN PROPELLER DAN INTERVAL  
TIP ROTOR TERHADAP EFISIENSI ROTOR PADA *MICRO  
QUAD-ROTOR* PADA KONDISI MELAYANG**

Georgius Suhud  
NRP. 4212 100 114

Dosen Pembimbing :  
Sutopo Purwono Fitri, S.T., M.Eng., Ph.D.  
Mizue Munekata, Ph.D.

JURUSAN TEKNIK SISTEM PERKAPALAN  
Fakultas Teknologi Kelautan  
Institut Teknologi Sepuluh Nopember  
Surabaya, Indonesia  
2016





**FINAL PROJECT – ME 141501**

***EFFECTS OF PROPELLER BLADE PROFILE AND ROTOR-TIP  
INTERVAL ON THE ROTOR EFFICIENCY OF A MICRO QUAD-  
ROTOR IN HOVERING***

Georgius Suhud  
NRP. 4212 100 114

Supervisors :  
Sutopo Purwono Fitri, S.T., M.Eng., Ph.D.  
Mizue Munekata, Ph.D.

DEPARTMENT OF MARINE ENGINEERING  
Faculty of Marine Technology  
Sepuluh Nopember Institute of Technology  
Surabaya, Indonesia  
2016

**LEMBAR PENGESAHAN**

**PENGARUH PROFIL DAUN PROPELLER DAN  
INTERVAL TIP ROTOR TERHADAP EFISIENSI ROTOR  
PADA MICRO QUAD-ROTOR PADA KONDISI  
MELAYANG**

**SKRIPSI**

Diajukan untuk Memenuhi Salah Satu Syarat Memperoleh  
Gelar Sarjana Teknik  
pada  
Bidang Studi *Marine Machinery and System* (MMS)  
Program Studi S-1 Jurusan Teknik Sistem Perkapalan  
Fakultas Teknologi Kelautan  
Institut Teknologi Sepuluh Nopember

Oleh:

**Georgius Suhud  
NRP. 4212 100 114**

Disetujui oleh  
Pembimbing Skripsi:

1. Sutopo Purwono Fitri, S.T., M.Eng., Ph.D. ( )  
NIP. 1975 1006 2002 12 1003
2. Mizue Munekata, Ph.D. ( )



SURABAYA  
JULI, 2016

**LEMBAR PENGESAHAN**

**PENGARUH PROFIL DAUN PROPELLER DAN  
INTERVAL TIP ROTOR TERHADAP EFISIENSI ROTOR  
PADA MICRO QUAD-ROTOR PADA KONDISI  
MELAYANG**

**SKRIPSI**

Diajukan untuk Memenuhi Salah Satu Syarat Memperoleh  
Gelar Sarjana Teknik

pada

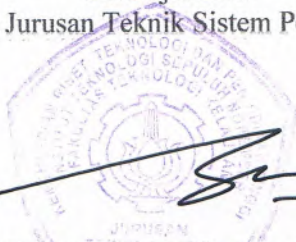
Bidang Studi *Marine Machinery and System* (MMS)  
Program Studi S-1 Jurusan Teknik Sistem Perkapalan  
Fakultas Teknologi Kelautan  
Institut Teknologi Sepuluh Nopember

Oleh:

**Georgius Suhud  
NRP. 4212 100 114**

Disetujui oleh

Ketua Jurusan Teknik Sistem Perkapalan



Dr. Eng. M. Badrus Zaman, S.T., M.T.  
NIP. 1977-0802 2008 01 1007

# **PENGARUH PROFIL DAUN PROPELLER DAN INTERVAL TIP ROTOR TERHADAP EFISIENSI ROTOR PADA MICRO QUAD-ROTOR PADA KONDISI MELAYANG**

**Nama Mahasiswa** : Georgius Suhud  
**NRP** : 4212 100 114  
**Jurusan** : Teknik Sistem Perkapalan  
**Dosen Pembimbing** : Sutopo Purwono Fitri, S.T., M.Eng.,  
Ph.D.  
Mizue Munekata, Ph.D.

## **Abstrak**

*Tujuan dari penelitian ini adalah untuk mengetahui pengaruh profil daun propeller dan interval rotor-tip terhadap aerodinamis termasuk efisiensi rotor pada kondisi melayang. Terdapat tiga tipe propeller yang digunakan. Semuanya dengan interval rotor-tip yang sama  $TI = 0.5R$ . Hanya untuk kasus propeller tipe 3 saja dimana  $TI$  divariasikan ( $TI = 1.0R$ ,  $0.5R$ , dan  $0.03R$ ). Batasan masalah pada studi ini adalah menganulir efek dinding – mengingat eksperimen dilakukan pada tempat yang luas. Gaya angkat, kecepatan rotor, serta konsumsi daya adalah variable-variable yang diukur untuk memperoleh data. Gaya angkat diukur menggunakan force gauge, kecepatan rotor diukur menggunakan tachometer, sedangkan konsumsi daya diperoleh melalui signal dari power supply. Pitch angle yang lebih kecil serta kecepatan rotor yang tinggi berkontribusi pada efisiensi aerodinamis terbaik.  $TI/R$  yang lebih lebar juga berkontribusi pada efisiensi rotor yang lebih baik.*

*Kata kunci: Micro quad-rotor, Micro UAV, efisiensi rotor, profil daun propeller, rotor-tip interval.*

*This page intentionally left blank*



# ***EFFECTS OF PROPELLER BLADE PROFILE AND ROTOR-TIP INTERVAL ON THE ROTOR EFFICIENCY OF A MICRO QUAD-ROTOR IN HOVERING***

**Student Name** : Georgius Suhud  
**Student ID Number** : 4212 100 114  
**Department** : Marine Engineering  
**Supervisor** : Sutopo Purwono Fitri, S.T., M.Eng.,  
Ph.D.  
Mizue Munekata, Ph.D.

## ***Abstract***

*The purpose of this research is to experimentally research how the propeller blade profile and different rotor-tip interval have effect to rotor efficiency at the hovering state. In this study, the effects of propeller blade geometry on aerodynamic characteristics included rotor efficiency of hovering quad-rotor are investigated experimentally. Three kinds of propellers are used and examined. All in the same distance of rotor-tip interval (TI) 0.5R. Only for the case of Type 3 propeller the TI is varied (TI = 1.0R, 0.5R, and 0.03R). The limit condition of this study is the negligible effect of the side wall – this is due to the experiments are performed in a large space. Lift, rotating speed of rotor and consumed power are measured in order to acquire data. The lift is measured by a force gauge, rotating speed of rotor is measured by a tachometer, while consumed electric power is obtained from the signal to the power of power supply. It is found that the smaller pitch angle and higher speed rotation contributes to the best aerodynamic efficiency. In addition, wider TI/R corresponds to better rotor efficiency also.*

*Keywords: Micro quad-rotor, Micro UAV, rotor efficiency, propeller blade profile, rotor-tip interval.*

*This page intentionally left blank*

## TABLE OF CONTENTS

<b>LEMBAR PENGESAHAN</b> .....	<b>i</b>
<b>ABSTRACT (INDONESIAN)</b> .....	<b>v</b>
<b>ABSTRACT (ENGLISH)</b> .....	<b>vii</b>
<b>FOREWORD</b> .....	<b>ix</b>
<b>TABLE OF CONTENTS</b> .....	<b>xi</b>
<b>LIST OF FIGURES</b> .....	<b>xiii</b>
<b>LIST OF TABLES</b> .....	<b>xv</b>
<b>CHAPTER I INTRODUCTION</b>	
1.1 Background .....	1
1.2 Experiment Place.....	2
1.3 Problem Statement .....	2
1.4 Objectives.....	3
1.5 Benefits.....	3
1.6 Problem Scope and Limitation .....	3
<b>CHAPTER II LITERATURE REVIEW</b>	
2.1 Micro quad-rotor .....	5
2.2 Propeller profile.....	6
2.3 Lift, Drag and Thrust.....	7
2.4 Lift coefficient ( $C_L$ ) .....	10

**CHAPTER III RESEARCH METHODOLOGY**

3.1 Experimental Flowchart ..... 13

3.2 Experimental Methods, Procedures, and Conditions ..... 14

    3.2.1 Experimental Methods ..... 14

    3.2.2 Experimental Procedures ..... 23

    3.2.3 Experimental Conditions ..... 24

3.3 Lift Measurement ..... 25

**CHAPTER IV DATA AND ANALYSIS**

4.1 Data Acquiring ..... 27

4.2 Data Analysis ..... 33

    4.2.1 Lift Performance ..... 34

    4.2.2 Hovering Efficiency ..... 36

**CHAPTER V CONCLUSION ..... 39**

**REFERENCES ..... 41**

**APPENDIX ..... 43**

## LIST OF TABLES

Table 1. Some quad-rotor projects .....	7
Table 2. Specification of test propellers .....	8

## LIST OF FIGURES

Figure 1. Maneuvers of micro quad-rotor .....	3
Figure 2. Forces acting on propeller blade .....	10
Figure 3. Induced velocity in the vicinity of a thrust generating rotor .....	12
Figure 4. Setting of equipment .....	16
Figure 5. Transmitter attached to PC.....	17
Figure 6. Force gauge sensor NIDEC SHIMPO FGP-1 .....	18
Figure 7. A micro quad-rotor as experiment object .....	18
Figure 8. Top view of micro quad-rotor.....	19
Figure 9. A schematic view of the experimental setup .....	20
Figure 10. Controller .....	21
Figure 11. DC Power Supply .....	22
Figure 12. A/D Converter Unit.....	22
Figure 13a. Waterpass on frame.....	23
Figure 13b. Waterpass on micro quad-rotor stem .....	23
Figure 14a. Interface of Servo Controller.....	27
Figure 14b. Notes is taken whenever changes in rotor speed occurs .....	28
Figure 15. Interface of data acquiring software.....	29
Figure 16. Saved converted signal data in .csv form.....	29
Figure 17. Example of data contents .....	30

Figure 18a. Force gauge program (1).....	31
Figure 18b. Force gauge program (2).....	32
Figure 18c. Force gauge program (3).....	32
Figure 19a. Lift coefficient ( $C_L$ ) vs rotor rotational speed ( $N$ ).....	34
Figure 19b. Lift coefficient ( $C_L$ ) vs rotor rotational speed ( $N$ ).....	35
Figure 20a. Consumed electric power per lift ( $P/L$ ) vs rotor rotational speed ( $N$ ) .....	36
Figure 20b. Consumed electric power per lift ( $P/L$ ) vs rotor rotational speed ( $N$ ) .....	37

# CHAPTER I

## INTRODUCTION

### 1.1 Background

In these recent years, the development of drone is becoming an emerging issue. This drone is classified as a Micro-UAV (Unmanned Aerial Vehicle). There are many kinds of the micro-UAVs. According to its utilization, this device is widely used in various areas including agricultural sector, photography and videos industry, topography obtaining data media, and so on. Such rotorcraft is controlled by wireless communication. One of the idea behind the initiation development of a multi-rotor helicopter is the principle of single-rotorcraft which is widely famed as helicopter. Just as what normal helicopter features, the most significant plus of this quad-rotor lays on its ability to take-off and land vertically. The helicopter has a fairly complicated system. For instance, in order to change the rotational speed of the propeller, pitch angle adjustment has to be conducted – this is what the complicated control system plays role at. In addition, helicopter is found difficult to flight in a small and complicated space due to its size. To cope with this issue, many researches and developments of micro quad-copter is still undergone.

Multi-rotor helicopter has the ability to move to all directions by means of just controlling rotational speed of each rotor – pitch angle control is not necessary. The experiment of the small body quad-rotor is a subject for this study. Due to the limitation of its body dimension, it is not possible for the quad-rotor to be mounted with large capacity of battery power. Hence, the flight duration of this small quad-rotor is short. This is the drawback of this micro quad-rotor.



The final objective in the future is to examine the best efficiency quad-rotor design amongst combinations. In this study, the effects of propeller blade geometry on aerodynamic characteristics included rotor efficiency of hovering quad-rotor are investigated experimentally. Three kinds of propellers are used and examined. All in the same distance of rotor-tip interval ( $TI$ )  $0.5R$ . Only for the case of Type 3 propeller the  $TI$  is varied ( $TI = 1.0R, 0.5R, \text{ and } 0.03R$ ). The limit condition of this study is the negligible effect of the side wall – this is due to the experiments are performed in a large space. Fluid force, rotating speed of rotor and consumed power are measured in order to acquire data. The fluid force is measured by a force gauge, rotating speed of rotor is measured by a tachometer, while consumed electric power is obtained from the signal to the power of power supply.

## 1.2 Experiment Place

This experiment and research was conducted in:

1. Fluid Machinery Laboratory, Department of Mechanical System Engineering, Faculty of Engineering, Kumamoto University, Japan.

## 1.3 Problem Statement

Blade types of propeller will most probably exhibit different aerodynamic characteristics even if installed in the same quad-rotor.

1. How is the rotor performance efficiency of the quad-rotor in case of propeller type 1, 2 and 3 installed?
2. How is the rotor performance efficiency of the quad-rotor in case of the variation of rotor-tip interval ( $TI$ )?
3. How do blade types effect on the quad-rotor aerodynamic characteristics?

## **1.4 Objectives**

From the problem statements above, the objectives of this report are:

1. To measure the lift acting and efficiency on the quad-rotor.
2. To identify whether types of propeller blade profiles have effect on the aerodynamic characteristics and the rotor performance efficiency.
3. To identify whether propeller-tip interval has effect on the aerodynamic characteristics and the rotor performance efficiency.

## **1.5 Benefits**

Benefits of conducting this experiment are:

1. By understanding and monitoring the aerodynamic characteristics on the micro-rotor blade types, the simulation and safe maneuvering can be conducted. Furthermore, this will effect on better response time (or completion elapsed time on a specific task of the rotor).
2. To understand the features of each propeller blades which later will result on the rotor performance of the quad-rotor.

## **1.6 Problem Scope and Limitation**

1. The quad-rotor which is used as object of experiment is based on A.R. Drone (P. J. Bristeau, et al., 2011)
2. The rotor 1 and rotor 3 is rotating clockwise, while rotor 2 and rotor 4 is rotating counter-clockwise.
3. Rotor speed is controlled by PC. The rotating speed is varied from 1500 RPM to 6000 RPM.
4. Negligible effect of side-wall. Experiments are performed in a large space.

5. The distance from the ground to the top of the rotor is defined as height  $h$  and maintained at the same 1400 mm (14.0R).

## **CHAPTER II**

### **LITERATURE REVIEW**

#### **2.1 Micro quad-rotor**

Micro quad-rotor belongs to unmanned aerial vehicles (UAVs). UAVs are subdivided into two general categories, fixed wing UAVs and rotary wing UAVs. Rotary winged crafts are superior to their fixed wing counterparts in terms of achieving higher degree of freedom, low speed flying, stationary flights, and for indoor usage (Gueaieb, 2010). Generally, two rotating propellers of the micro quad-rotor rotate clockwise whereas on the other hand, two others rotate counter-clockwise. This mechanism results to generate lift.

This paper is working on experimenting rotating wing micro quad-rotor. The details about the micro quad-rotor which is used as the object of the experiment will be explained in Chapter 3. However, in this chapter, the concept and fundamental of the micro quad-rotor is discussed.

There are four maneuvers that can be accomplished by changing the rotational speed of each rotor (Gueaieb, 2010). These four maneuvers are illustrated in Figure 1. Those maneuvers are:

1. Altitude

Altitude maneuver means increasing and/or decreasing lift so that micro quad-rotor soars and/or lowers into designated position.

2. Yaw

Yaw maneuver means that the micro quad-rotor is spinning on the point of origin axis. This maneuver is achieved through changing the rotation speed between clockwise and counter-clockwise rotating propellers.

### 3. Pitch

Pitching is a mechanism which makes micro quad-rotor trim to the front side or to the rear side. This maneuver is controlled through changing the relative speeds of the front and rear rotors.

### 4. Roll

Roll is accomplished through changing the relative speed of the right and left propellers.

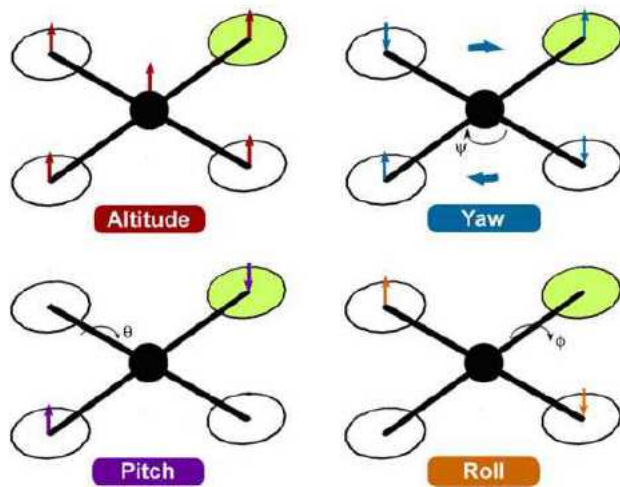






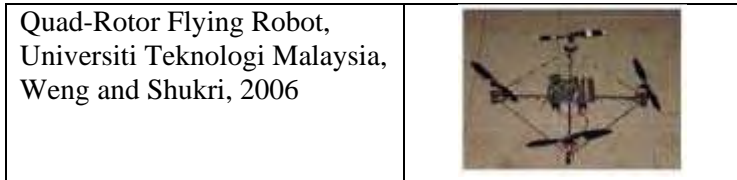


Figure 1. Maneuvers of micro quad-rotor  
(Source: Gueaieb, 2010)

Table below shows some other quad-rotor projects which already conducted.

Table 1. Some quad-rotor projects

Project	Picture
STARMAC, Stanford University, Waslander et al., 2005	
OS4, EPFL, Bouabdallah, 2006	
Pennsylvania State University, Hanford, 2005	
Helio-copter, Brigham Young University, Fowers, 2008	
HMX-4, Pennsylvania State University, Altug et al., 2002	
Quad-Rotor UAV, University of British Columbia, Chen and Huzmezan, 2003	






Source: Gueaieb, 2010

## 2.2 Propeller profile

The aerodynamic characteristics of three kinds of propeller profile are investigated. The specifications of propeller profile are shown in Table 2.

Table 2. Specifications of test propeller

Type		TI/R [-]	R [mm]	$\alpha_{0.7}$ [°]	$l_{0.7}$ [mm]
Type 1 (APC)		0.5	127	12.0	21.9
Type 2 (enRoute)		0.5	120	9.6	16.7
Type 3 (AR Drone)		1.0 ; 0.5 ; 0.03	100	21.0	16.3

Type 1 is the standard propeller for a multi-copter, made by APC. Type 2 is the propeller installed in Zion PG400 made by enRoute corporation. Type 3 is the propeller installed in AR. Drone made by Parrot Inc. The rotor radius  $R$ , the pitch angle at the non-dimensional local radius  $r/R = 0.7$  ( $\alpha_{0.7}$ ), and the cord length at  $r/R = 0.7$  ( $l_{0.7}$ ), are shown in Table 1. The coordinate system  $x$ ,  $y$ , and  $z$  are shown in Figure 8 and Figure 9. The lift becomes bigger as the pitch angle ( $\alpha$ ) at  $r/R = 0.7$  increases, if not stall. Therefore, the lift of Type 3 is the highest.

### 2.3 Lift, Drag and Thrust

There are three kinds of forces acting on the propeller blade: lift, drag, and thrust. The details of these forces are illustrated in Figure 2.

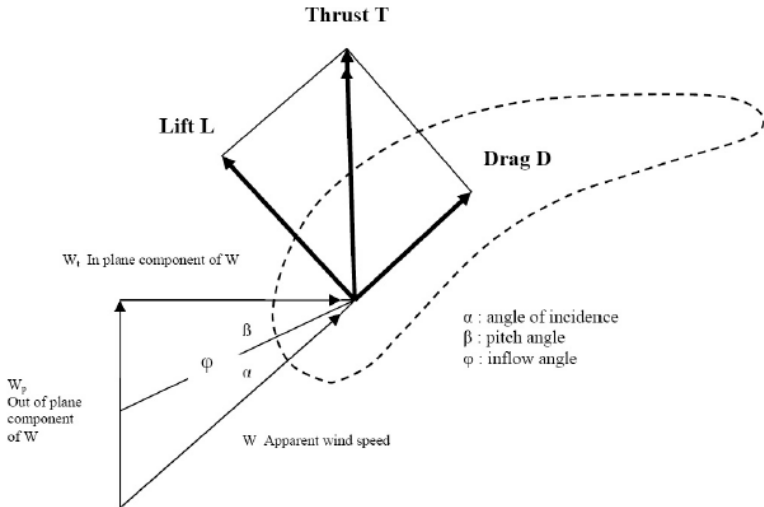


Figure 2. Forces acting on propeller blade

The lift force  $L$  arises in a direction that is perpendicular to the air stream. According to the Bernoulli Effect, the top part of the airfoil has higher stream velocity compared to the lower one. Thus resulting to the lower pressure. Since the lower part of the airfoil has higher pressure than the top part, the lift is generated. The lift equation is described altogether with the lift coefficient  $C_L$  on Chapter 2.4.

Drag force  $D$  is described by the drag coefficient  $C_D$



$$C_D = \frac{2D}{\rho S V_T^2}$$

The lift  $L$  and drag  $D$  forces vary with the angle that the rotor blade makes with the direction of the air stream designated as the angle of attack  $\varphi$ .

The resultant of the lift and drag forces constitutes the thrust force  $T$  that effectively rotates the rotor blade. The resultant ratio of lift to drag  $L/D$  ratio is a function of the angle of attack  $\varphi$  for a given airfoil section (Ragheb, 2013).

According to the study conducted by Tata Sudyanto in 2009, momentum theory provides insight to the mechanism of how the rotor generates thrust as it accelerates (or decelerates) some amount of air mass in the process.

For steady flow along the flow field, the mass flow is constant at any point of observation.

$$\frac{dm}{dt} = \rho A_0 w_0 = \rho A_1 w_1 = \rho A_2 w_2$$

$$A_1 = \pi (R^2 - r_{root}^2)$$

The total thrust exerted by each accelerating air particle in the control volume is

$$\begin{aligned} T &= \int_{w_0}^{w_2} \frac{dm}{dt} dw \\ &= \int_{w_0}^{w_2} \rho A_1 w_1 dw \\ &= \rho A_1 w_1 (w_2 - w_0) \end{aligned}$$

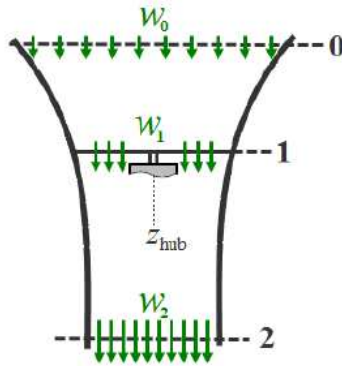


Figure 3. Induced velocity in the vicinity of a thrust generating rotor

## 2.4 Lift coefficient ( $C_L$ )

The lift coefficient hovering efficiency is defined by the following formula.

$$C_L = \frac{2 L}{\rho S V_T^2}$$

Where  $\rho$  is the density of air,  $S$  is the rotation area of the quad-rotor and  $V_T$  is the averaged rotor tip speed.  $S$  is defined according to the following formula.

$$S = n \pi R^2$$

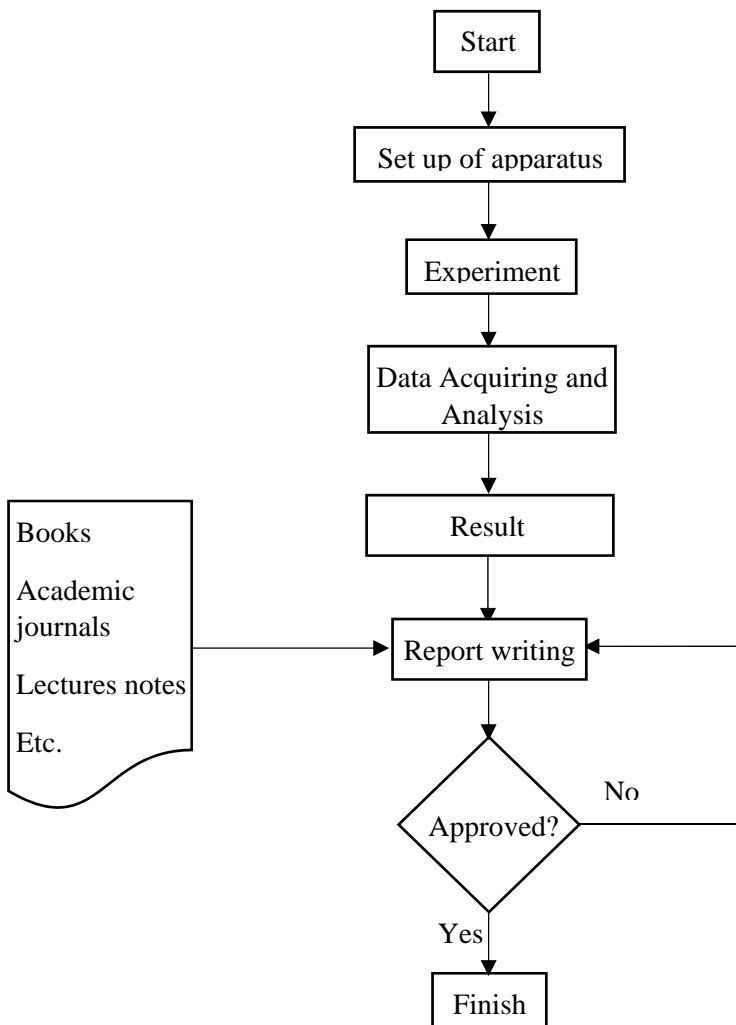
Where  $n$  is the number of rotor. In this case  $n$  is 4.  $R$  is the rotor radius.  $V_T$  is defined by the following formula.

$$V_T = \frac{\pi N R}{30}$$

Where  $N$  is the rotor speed (RPM). The consumed electric power of quad-rotor is simultaneously measured. The hovering efficiency is evaluated through the consumed electric power per unit lift.

# CHAPTER III RESEACRH METHODOLOGY

## 3.1 Experimental Flowchart



## 3.2 Experimental methods, procedures, and conditions

### 3.2.1 Experimental methods

This paper is mainly written based on the experiment conducted on the micro quad-rotor. Every time after experiment was finished, the data was acquired in a digital signal form using AD Converter (*Analog Digital converter*). The next step is converting the data into the Microsoft excel form using a C-language programming-based software. After the data is converted, the excel data are combined and represented in graphic figures using a program called “*Sma4Windows*”. After the figures are finished, the report is written with books, academic journals, lecture notes, and any other reliable sources.

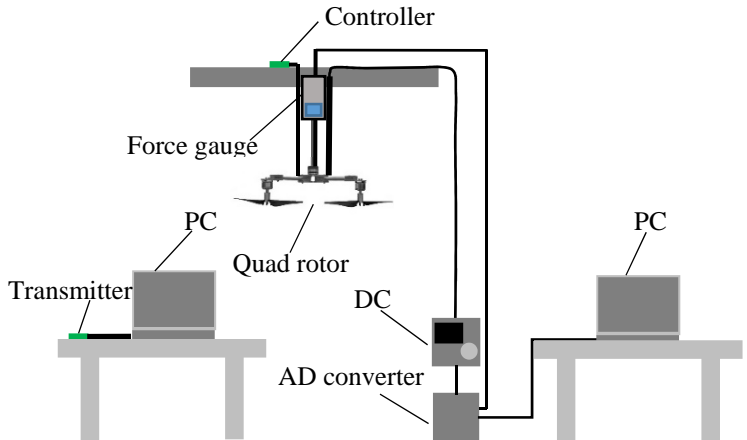


Figure 4. Setting of equipment

As shown in Figure 4, it can be observed that there are some equipment that are used during the experiment:

1. Transmitter

Transmitter sends command data from the PC in order to control the rotating speed of the micro quad-rotor. The software which was used during the experiment is “*ServoController*”. The transmitter is “*XBee 62*”.

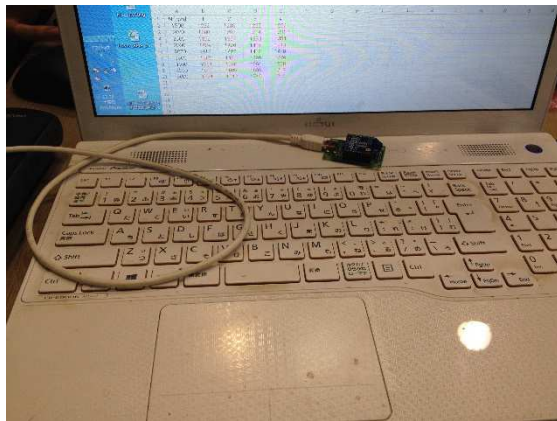


Figure 5. Transmitter attached to PC

2. PC

During the experiment, at least one PC (usually two) should be used to transmit the command of controlling rotating speed, as well as plays role as data receiver.

### 3. Force gauge

Force gauge is used to measure the lift generated by the micro quad-rotor. In case of FGP-1, the measured lift is the actual lift. However, in case of FGP-5, the measured lift should be times with the value of 5 to obtain the actual lift. All lift is measured in gram force (gf) unit.



Figure 6. Force gauge sensor NIDEC SHIMPO FGP-1

#### 4. Micro quad-rotor

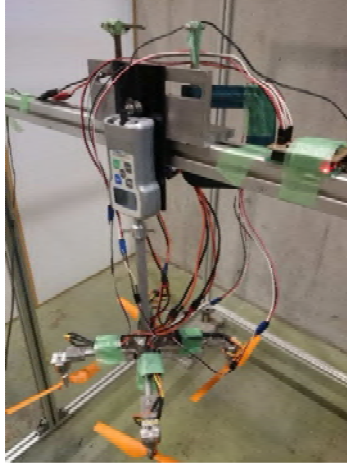


Figure 7. A micro quad-rotor as experiment object

The quad-rotor used in this study is based on AR. Drone made by Parrot Inc (Tsuji, et al., 2014). During the measurement, the body cover and sensors are removed from the quad-rotor in order to eliminate the influence of them on the rotor wake.



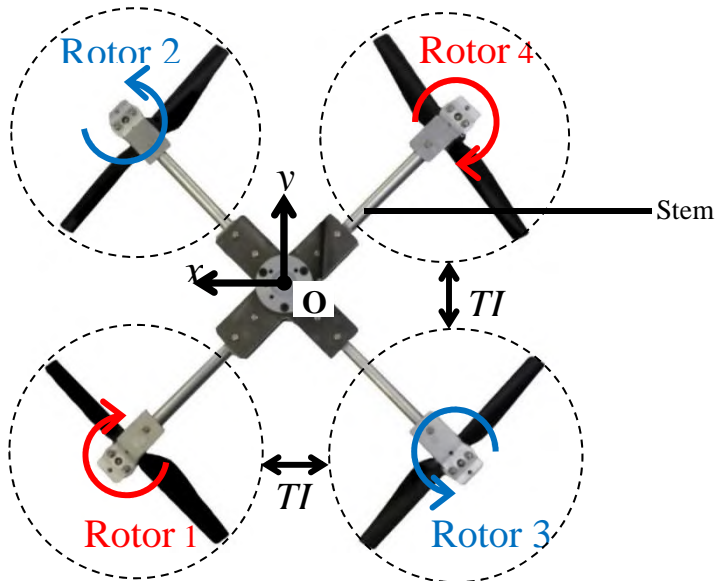


Figure 8. Top view of micro quad-rotor

Figure 8 shows the top view of the micro quad-rotor. As shown in Figure 9, it can be examined that the center body of the quad rotor is fixed to a support cane. This cane is fastened to the upper rigid frame using flanges. The distance from the ground to the top of the rotor is maintained at the  $h$  1400 mm. The rotor height is out of the ground effect.

The quad-rotor has four rotors in a cross configuration, and each rotor has a pair of blades. The rotor radius  $R$  is 100 mm. The minimum distance between the rotor tip is  $0.5R$ . The rotor number 1 and number 3 rotate clockwise, while rotor number 2 and number 4 rotate counter-clockwise respectively. The rotor speed is controlled by a wireless PC and is kept in hovering state

condition. Typically the range of rotor speed (RPM) is different of each propeller type. However, the rotor rotational speed tuned around  $N = 3270$  rpm (revolutions per minute) in order to provide the lift of  $100 \pm 2$  gf. The distance from the ground to the top of the rotor is maintained at the rotor height  $h = 1400$  mm ( $14.0 R$ ).

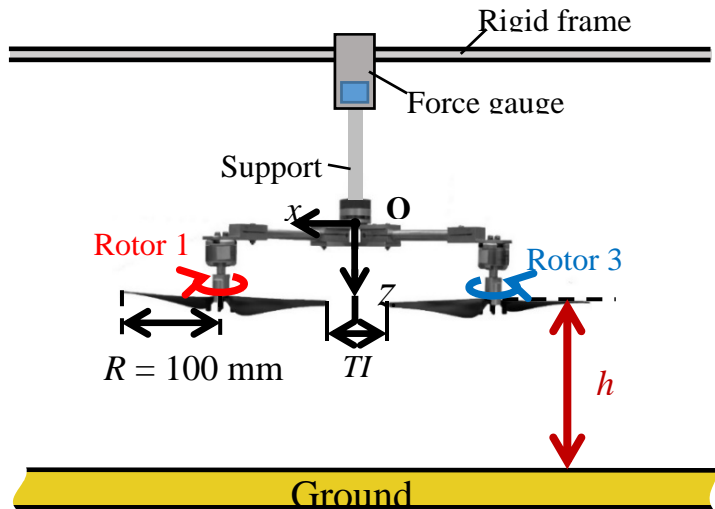


Figure 9. A schematic view of the experimental setup

##### 5. Controller

Cables from each rotor is attached to the controller as shown in figure below. In addition, a jack-cable is attached to the force gauge sensor so that the data can be transferred directly to the PC. The same also apply to the tachometer.

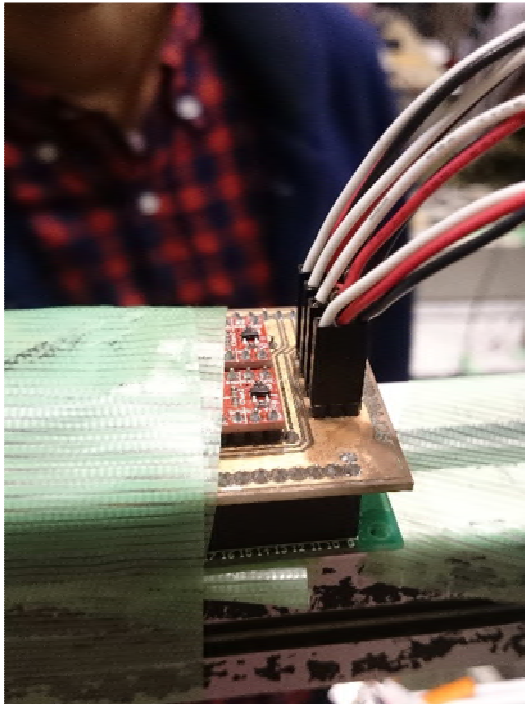


Figure 10. Controller

6. DC power supply

The source of electrical power is indicated in the “*Kenwood DC Power supply*”. The default value of voltage should be 12.01 V and the default value of the current should be 0.18 A.

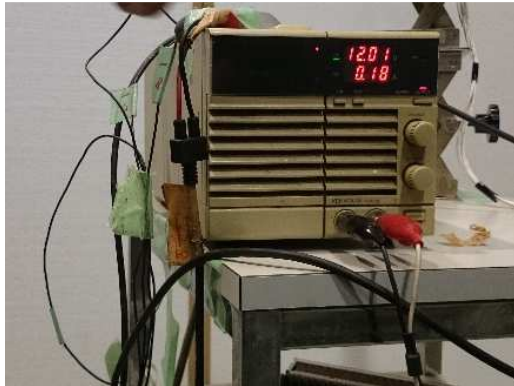


Figure 11. DC Power supply

#### 7. AD converter unit

AD converter stands for analog/digital converter. This converter is connected to a PC for data acquiring.



Figure 12. A/D converter unit

## 8. Waterpass

This equipment is for ensuring the media is precisely horizontal (flat). The waterpass is used both for ensuring the perfectly horizontal position for the frame as well as the stem of the micro quad-rotor.

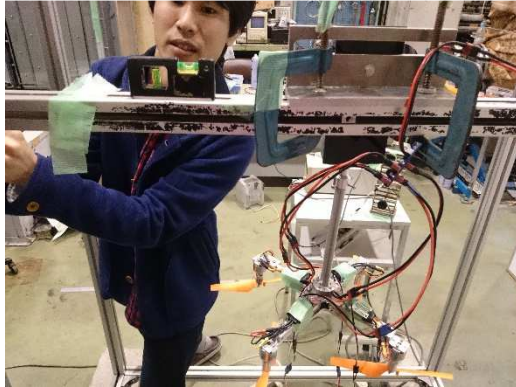


Figure 13a. Waterpass on frame



Figure 13b. Waterpass on micro quad-rotor stem

### 3.3.2 Experimental procedures

The experiment is generally classified into two experiments. Fundamentally, both experiments are the same. The final objective of both experiments is to identify the efficiency of micro quad-rotor in hovering condition. The first experiment is about the variation types of propeller profile. While the second one is varying the tip-interval distance of propeller Type 3. However, the steps of experiment are likely the same. The details of the experiment are as follows:

1. Preparing the frame.

The frame is equipped with 1500 mm rulers on both sides of the frame. The frame is set at a certain height first. For this experiment, height is maintained at 1400 mm above the ground. The alignment of the top frame is checked with the waterpass – ensuring that the frame is perfectly flat (see Figure 13a).

2. Preparing the micro-quad rotor body.

For the propeller blade profiles experiment, the rotor is attached with the propeller Type 1 first, with propeller Type 2 and 3 are fitted consecutively as soon as experiment of propeller each type finished. While in tip-interval variation experiment, the micro quad-rotor stem with several length types (i.e.  $TI/R = 0.03, 0.5$  and  $1.0$ ) are installed consecutively after each experiment for each tip-interval is finished. Every time the stem is installed, two units of waterpass are employed to ensure that the center part as well as the edge part of the micro-quad rotor body is well-aligned.

3. Connecting micro quad-rotor body with upper rigid frame.

The micro quad-rotor body is fastened to the upper rigid frame using flanges. The lower flange connects cane with the body of the micro quad-rotor. While the upper flange connects cane with the force gauge.

4. Plugging all cables to the designated places.  
The cables from each rotor are plugged to the controller. Power cables for each rotor are connected to the DC power supply. The cable from force gauge as well as cables measuring current, voltage and rotating speed are connected to the A/D converter unit.
5. Running the experiment.  
While running the experiment, the rotating speed of each rotor is controlled using “*ServoController*” software. The rotating speed is also manually measured using tachometer in order to acquire the deviation data. The A/D converter unit is connected to the PC as well as to the cables measuring current, voltage, rotor speed, and lift. For each rotor speed variation, two samples of these data are taken. While acquiring data, only two inputs are possible, so changing of cable combination was needed to perform.

### 3.3.3 Experimental conditions

- The quad-rotor which is used as object of experiment is based on A.R. Drone (P. J. Bristeau, et al., 2011)
- For propeller profile experiment : Three kinds of propellers are used and examined. All with the same tip interval 0.5R.

- For rotor-tip interval experiment: Object propeller only Type 3. Tip interval are 0.03R, 0.5R, 1.0R.
- Rotor 1 and 3 rotate clockwise, Rotor 2 and 4 rotate counter-clockwise.
- Rotating speed is varied from 1500 RPM to 6000 RPM.
- Negligible effect of side-wall – experiments are performed in a large space.
- The distance from ground to the top of rotor is defined as  $h$  and maintained at 1400 mm.

### 3.3 Lift measurement

The lift ( $L$ ) is measured by a force gauge sensor (NIDEC SHIMPO FGP-5) as shown in Figure 6. The detail specification of this equipment can be examined in the appendix section. In term of the accuracy of this equipment, the equipment has an accuracy of  $\pm 0.2\%$  Capacity (R.C.) – around  $\pm 5.000$  kgf or  $\pm 10$  lbf and  $\pm 1/2$  digit ( $23^\circ\text{C}$ ) The measurement data by force gauge are sampled by 20 kHz. Sampling period (time average) is 40 seconds. The time averaged lift  $L$  is obtained by ensemble average.



*This page intentionally left blank*

## CHAPTER IV DATA AND ANALYSIS

### 4.1 Data acquiring

As illustrated in Figure 14a, a software is employed as a media to control the micro quad-rotor rotating speed. Below is the interface of the software.



Figure 14a. Interface of ServoController

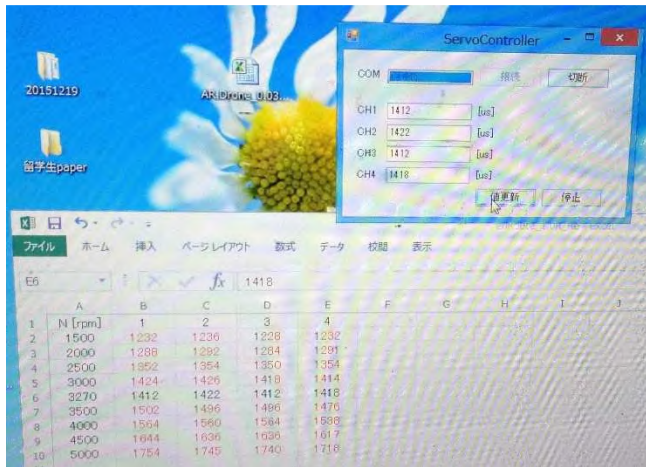


Figure 14b. Notes is taken whenever changes in rotor speed occurs

The *ServoController* unit is in Hz. Figure 14b exhibits how is the configuration of each rotor speed in ( $\mu\text{s}$  or MHz). In addition, the “COM” means the input computer source where the transmitter is attached at.

Regarding to the data acquiring, another software is employed. The interface of the software is as Figure 15 below. For each rotor speed, two samples of data were taken. Each with the combination as follows: Lift and voltage; rotor speed and current. This sampling period is 40 seconds. The original data showed in the form of signal diagrams. Therefore, in order to make the data can be processed, the data is then saved as “.csv” (Microsoft Excel) format.

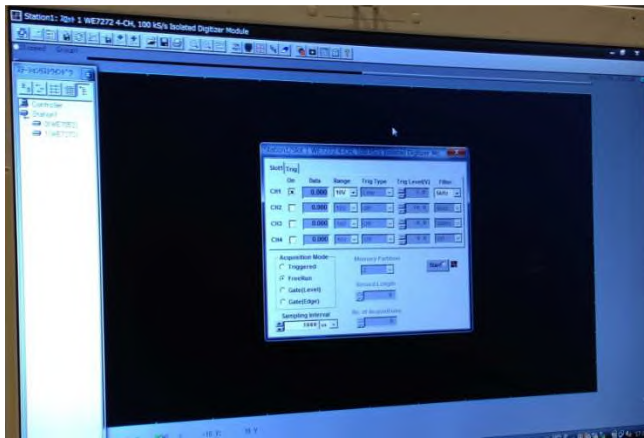


Figure 15. Interface of data acquiring software

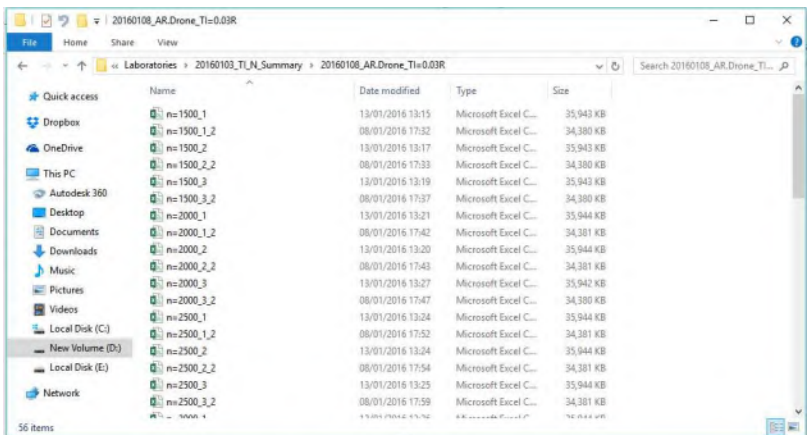


Figure 16. Saved converted signal data in .csv form

Excel interface showing a spreadsheet with data. The spreadsheet has columns A through J and rows 1 through 21. The data is as follows:

	A	B	C	D	E	F	G	H	I	J
1	Model	WE7271								
2	BlockNum	1								
3	BlockSize	800000								
4	Date	08/01/2016								
5	Time	19:28:24								
6	TraceNam	CH1	CH2							
7	VUnit	V	V							
8	HResoluti	5.00E-05	5.00E-05							
9										
10	block0									
11	0.00E+00	1.06E-02	1.11E+00	2.89E-01	2.38E-02					
12	5.00E-05	1.03E-02	1.04E+00	1.82E-01	1.55E-02					
13	1.00E-04	1.08E-02	1.15E+00	9.04E-02	1.73E-02					
14	1.50E-04	1.16E-02	1.31E+00	1.75E-01	2.20E-02					
15	2.00E-04	1.13E-02	1.30E+00	3.53E-01	1.92E-02					
16	2.50E-04	1.13E-02	1.27E+00	3.86E-01	2.32E-02					
17	3.00E-04	1.10E-02	1.21E+00	3.37E-01	2.38E-02					
18	3.50E-04	1.04E-02	1.08E+00	2.74E-01	2.17E-02					
19	4.00E-04	1.02E-02	1.05E+00	1.59E-01	2.45E-02					
20	4.50E-04	1.11E-02	1.21E+00	1.07E-01	1.05E-02					
21	5.00E-04	1.16E-02	1.32E+00	2.63E-01	2.35E-02					
	A	B	C	D	E	F	G	H	I	J
799990	4.00E+01	1.34E-02	1.27E+00	3.20E-01	4.95E+00					
799991	4.00E+01	1.30E-02	1.19E+00	2.92E-01	4.95E+00					
799992	4.00E+01	1.26E-02	1.07E+00	1.72E-01	4.94E+00					
799993	4.00E+01	1.23E-02	1.10E+00	1.01E-01	4.94E+00					
799994	4.00E+01	1.33E-02	1.26E+00	2.24E-01	4.94E+00					
799995	4.00E+01	1.35E-02	1.35E+00	3.83E-01	4.94E+00					
799996	4.00E+01	1.33E-02	1.29E+00	3.71E-01	4.94E+00					
799997	4.00E+01	1.33E-02	1.26E+00	3.19E-01	4.94E+00					
799998	4.00E+01	1.27E-02	1.15E+00	2.59E-01	4.94E+00					
799999	4.00E+01	1.24E-02	1.06E+00	1.33E-01	4.94E+00					
800000	4.00E+01	1.27E-02	1.14E+00	1.37E-01	4.94E+00					
800001	4.00E+01	1.35E-02	1.31E+00	3.12E-01	4.94E+00					
800002	4.00E+01	1.33E-02	1.32E+00	4.06E-01	4.95E+00					
800003	4.00E+01	1.33E-02	1.26E+00	3.44E-01	4.95E+00					
800004	4.00E+01	1.31E-02	1.21E+00	2.93E-01	4.94E+00					
800005	4.00E+01	1.25E-02	1.08E+00	1.78E-01	4.95E+00					
800006	4.00E+01	1.22E-02	1.03E+00	7.15E-02	4.94E+00					
800007	4.00E+01	1.29E-02	1.19E+00	1.72E-01	4.95E+00					
800008	4.00E+01	1.34E-02	1.32E+00	3.45E-01	4.94E+00					
800009	4.00E+01	1.34E-02	1.30E+00	3.73E-01	4.95E+00					
800010	4.00E+01	1.33E-02	1.28E+00	3.27E-01	4.95E+00					

Figure 17. Example of a data contents

The first column is the sampling period in seconds. From 0 to 40 seconds with increment of 0.00005 seconds. The second column is the lift measured in each sampling period. The third is the voltage. The fourth is the current. And lastly is the rotor speed.

It can be examined in the Figure 17 above that the number of data is a lot. Therefore, a C-language programming application is needed. The software is named as “*Force\_gauge*”.

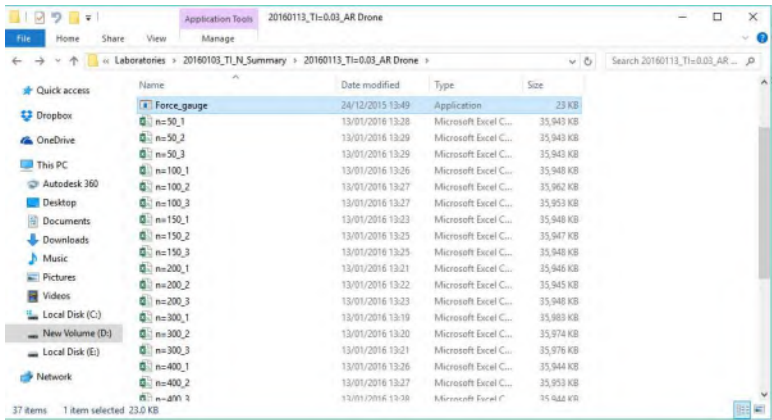


Figure 18a. Force gauge program (1)

The interface of the *Force\_gauge* program is as follows. The usage of this program is to combine all the excel data from rotor speed equals 1500 to 6000 RPM.

Take “*offset\_in*” data as example. The steps are as follows:

1. Number of data point(s) input. Here the value in the Microsoft excel is -0.00425 kgf. However, the unit of the program here is in gf, hence, the value of -4.25 should be input.

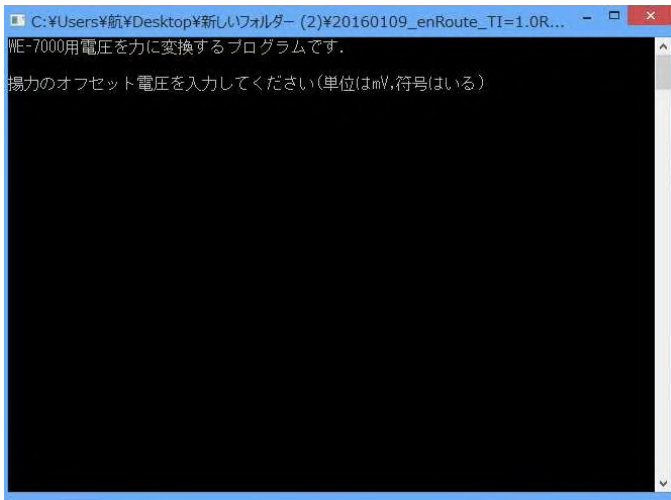


Figure 18b. Force gauge program (2)

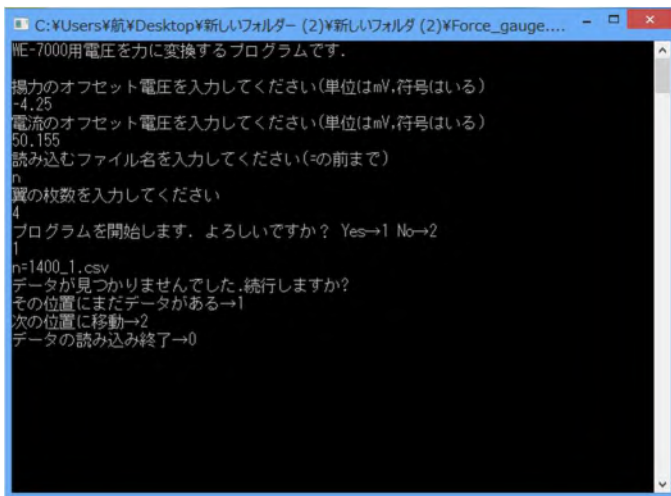


Figure 18c. Force gauge program (3)

2. Next is asking about the value of the current. In this case, the value is 0.050155153 A. However, the unit of the program is in mA, hence, the value of 50.155 should be input.
3. The program is asking what is the first character of the Microsoft excel data name. In this case, “n” is input.
4. This is asking about how many is the propeller number. The value of “4” should be inserted.
5. The calculation is started. To calculate all type “2”.
6. Calculation is finished. Please type the name the files would be saved as.

After the data is finished, the software “*Sma4Windows*” is used to make graphs.

## **4.2 Data analysis**

For quad-rotor, the four wakes close each other due to the interference of 4-rotor wake. This phenomena is further studied by Tobo et al. in 2015, while regarding of the propeller profile Mitsuzaki et al. in 2015 also. In this study effect of propeller profile on the efficiency of hovering of the micro-quad rotor is investigated.



### 4.2.1 Lift performance

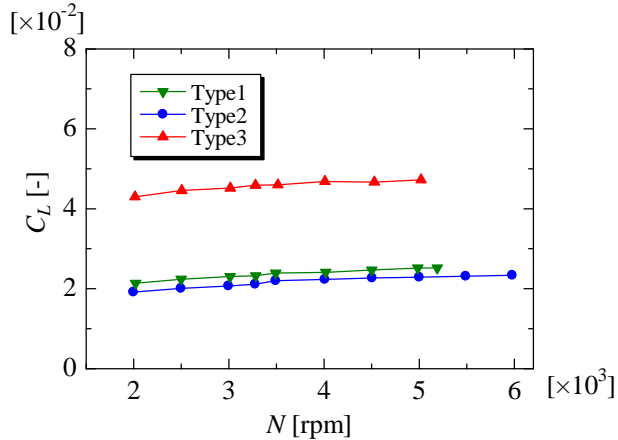


Figure 19a. Lift coefficient ( $C_L$ ) vs rotor rotational speed ( $N$ )

Figure 19a shows the lift coefficient ( $C_L$ ) vs the rotating speed ( $N$ ). The lift in all Types increases slightly with the increase of rotating speed until it reaches maximum rotating speed of each propeller. The lift coefficient ( $C_L$ ) of Type 3 is the largest. When the rotating speed is equal to 5000 rpm, the lift coefficient ( $C_L$ ) of Type 2 is 9.1% less than that of Type 1. The  $C_L$  of Type 3 is 88% larger than that of the Type 1. The pitch angle of Type 3 is the largest of all. According to the study conducted by Song in 2009, this study shows that as the pitch angle is greater, the lift generated is also greater.

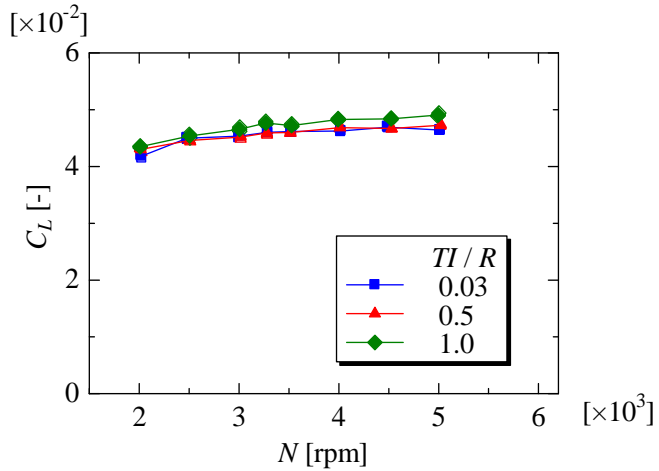


Figure 19b. Lift coefficient ( $C_L$ ) vs rotor rotational speed ( $N$ )

Figure 19b shows that lift coefficient ( $C_L$ ) increases slightly with the increase of the rotating speed ( $N$ ). The lift coefficient ( $C_L$ ) increases with increasing of rotor interval. The lift coefficient of  $TI/R = 1.0$  is slightly the highest amongst all. At the rotating speed of  $N = 5000$  rpm, the lift coefficient ( $C_L$ ) of  $TI/R = 0.03$  is lower than that of the  $TI/R = 0.5$ . While the lift coefficient ( $C_L$ ) of  $TI/R = 1.0$  is higher than that of the  $TI/R = 0.50$ . As the air inflow through each rotor increases, the rotor-tip interval ( $TI$ ) is smaller, and the wake interference is higher. Vice versa. If  $TI$  is larger, the wake interference is smaller. When the wake interference occurs, the axial momentum decreases. However, if the axial momentum is larger, the lift generated is also getting larger.

## 4.2.2 Hovering efficiency

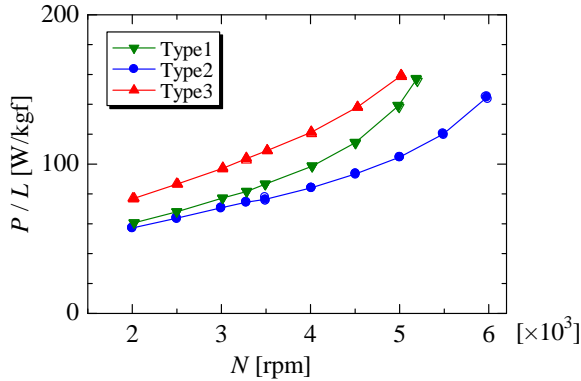


Figure 20a. Consumed electric power per lift ( $P/L$ ) vs rotor rotational speed ( $N$ )

Figure 20a shows consumed electric power per lift ( $P/L$ ) vs rotating speed ( $N$ ).  $P/L$  is increased with increasing of  $N$  regardless of propeller profile. The  $P$  in the  $P/L$  stands for the consumed electric power to rotate rotors and generate lift ( $L$ ). The consumed electric power due to rotate motors without rotors is subtracted from the consumed electric power applied to  $P$ . The  $P/L$  means the hovering efficiency and the value of  $P/L$  decreases with the higher hovering efficiency. When rotating speed equals to 5000 rpm,  $P/L$  of Type 2 is 25% lower than Type 1. And  $P/L$  of Type 3 is 14% higher than Type 1. In general attack angle (pitch angle) of wind is larger, the drag force is larger (Song, 2009). The pitch angle of Type 3 is the largest amongst all propellers. The drag force of Type 3 is also the largest of all propellers. As a result, the axial torque of motor needed to rotate the propeller is larger on Type 3. And the consumed electric power increases and the hovering

efficiency decreases. While the pitch angle of Type 2 is the smallest and consumed electric power is low. It is ineffective for the propeller with small pitch angle to reduce the drag, that is, to reduce the consumed electric power. It needs for the rotor reduced the drag to generate high lift. Consequently we conclude that the propeller with small pitch angle applied to the high speed rotor provides the higher efficiency of hovering.

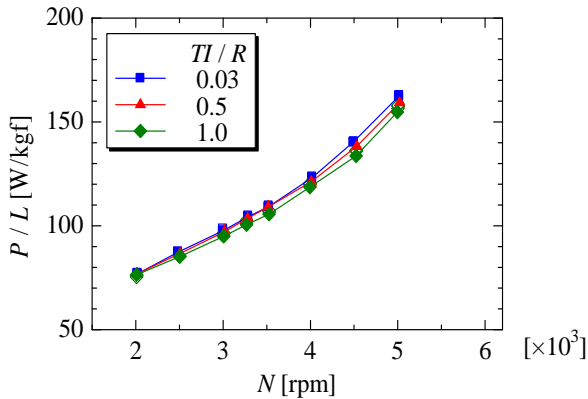


Figure 20b. Consumed electric power per lift ( $P/L$ ) vs rotor rotational speed ( $N$ )

Figure 20b shows consumed electric power per lift ( $P/L$ ) increases proportionally with the increasing of rotating speed ( $N$ ). As the rotor-tip interval ( $TI$ ) is getting wider,  $P/L$  is going down. For the  $TI/R = 1.0$ , the  $P/L$  is the lowest among all. At the rotating speed of  $N = 5000$  rpm, the  $P/L$  of  $TI/R = 0.03$  is 2% higher than that of the  $TI/R = 0.5$ . The  $P/L$  of  $TI/R = 1.0$  is 2.8% lower than that of the  $TI/R = 0.5$ . The hovering efficiency is based on the value of  $P/L$ . The smaller the value of  $P/L$  corresponds to the higher value of hovering efficiency. Study conducted by Tsuji in 2014 shows that the smaller value of  $TI/R$  corresponds to higher hovering efficiency

$(P/L)$ . Therefore,  $TI/R = 1.0$  is the best hovering efficiency amongst all rotor-tip intervals ( $TI$ ).

## **APPENDIX**

**APPENDIX A:  
TECHNICAL SPECIFICATION OF EQUIPEMENT**



color : Silver

※Purple color is for Japanese model.

- 

### Download the data to Excel with high speed

- Add-in software "Toriemon USB" enable us to download the data with 100 times per second. Efficiently edit the data on the PC. You can download ""Toriemon USB"" from our website free of charge.

- **High-speed sampling**

- It is possible to download the data on high speed with sampling rate of 1000 times per second.

- **Memory function is available**

- Three memory mode; Continuous memory, Single memory and Standard memory. Memory capacity; 1000 data in Continuous memory mode.

- **USB Communication feature**

- Incorporate the high versatility USB into the interface. It's easy to download the data in communicate with PC.

- **Comparator function**

- Available judgment of acceptance for measuring value with high/low limit setting.
- Wide variation with the motorized test stand.

## Specifications

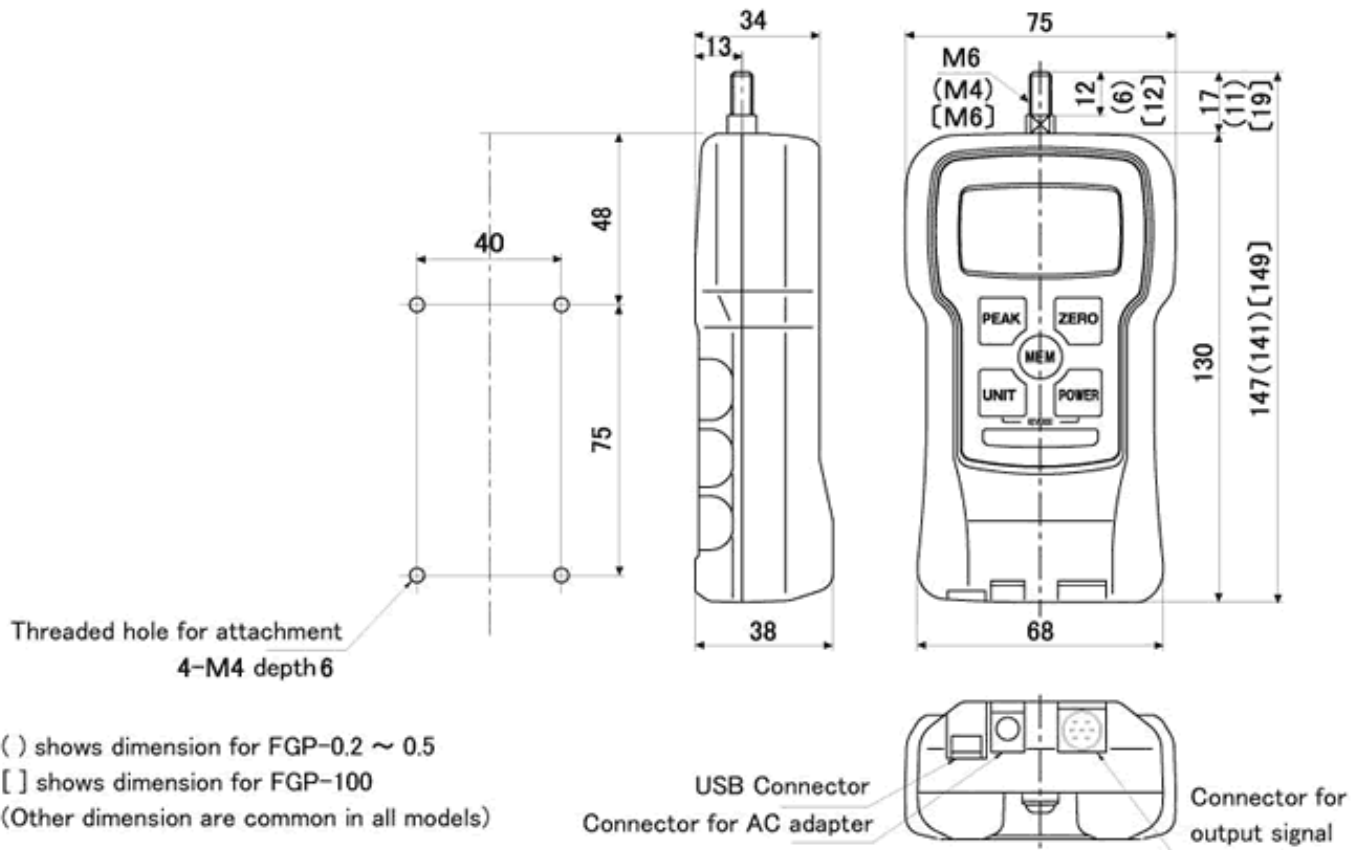
Model	FGP-0.2	FGP-0.5	FGP-1	FGP-2	FGP-5	FGP-10	FGP-20	FGP-50	FGP-100
Capacity(R.C.)	±2.000N (±200.0g)	±5.000N (±500.0g)	±10.00N (±1000g)	±20.00N (±2.000kg)	±50.00N (±5.000kg)	±100.0N (±10.00kg)	±200.0N (±20.00kg)	±500.0N (±50.00kg)	±1000N (±100.0kg)
	(±0.5lb)	(±0.1lb)	(±0.2lb)	(±5lb)	(±10lb)	(±20lb)	(±50lb)	(±100lb)	(±200lb)
Display range	±2.000N ±200.0g	±5.000N ±500.0g	±10.00N ±1000g	±20.00N ±2000g	±50.00N ±5.000kg	±100.0N ±10.00kg	±200.0N ±20.00kg	±500.0N ±50.00kg	±1000N ±100.0kg
	±0.5lb	±0.1lb	±0.2lb	±5lb	±10lb	±20lb	±50lb	±100lb	±200lb
Resolution	0.001N		0.01N	0.01N	0.01N	0.1N		0.1N	1N
	0.1g		1g	0.001kg	0.001kg	0.01kg		0.01kg	0.1kg
	0.001lb		0.001lb	0.001lb	0.01lb	0.01lb		0.1lb	0.1lb
Unit	N,kg(g),lb(oz)(Reversible display)								
Measuring mode	Standard measuring,Plus peak measuring,Minus peak measuring								
Display cycle	1,2,3,5,10,20 times per second								
Sampling Rate	1000 times per second								
Accuracy	±0.2% R.C. ±1/2digit(23°C)								
Influence of temperature	Gain:±0.01%LOAD/°C Zero:±0.01%/R.C./°C(Drift of zero point can be cancelled with tracking function.)								
	Main display:4-digits 12mm high, Reversible display								
	Unit display:3-digits 7mm high								



Display	Other display 1."LO BAT"(Decrease battery voltage), 2."BAT"(Battery charge), 3."OVR"(Over load), 4."Peak"(Peak hold mode)	
Overload	200%R.C.	150%R.C.
Tracking	Available(ON/OFF)	
USB	Communicate with PC by special application software(maximum 100 times per second). Connection cable is standard accessory.	
RS-232C	Communicate with PC by special command(maximum 100 times per second), Connection cable is option.	
Output	Analog	±1V, Accuracy ±50mV, through a 12 bit D/A converter, Output update 1000 times per second, Acceptable tare, Load resistance is more than 10k Ω
Overload/ Comparator	Open-collector output(Max DC30V/5mA).Either overload output or comparator output.	
Power	Rechargeable Nickel hydride battery or AC adapter/charger, Measurable during the charge, Operating hours:about 8 hours after full charge, Charging time: Max 16 hours(when the battery is full, charge is finished automatically.)	
Auto Power Off	10 minutes (not active if adapter/charge is in use) or OFF	
Memory function	Continuous memory: 1000 data, Single memory: 100 data, Standard memory: 50 data Statistic function(max, minimum, peak, average, standard deviation)	
Comparator function	Yes(high and low)	
Temperature range	0-40°C no condensation	
Humidity range	35 ~ 85%RH no condensation	
Dimensions	147mm *(L)×75mm(W)×38mm(H)	
Weight	Approx.450g	Approx.500g
Accessories (Included)	AC adapter/charger, carrying case, hook, chisel, flat head, notched head, hanger, cone head, extension rod, USB cable	
Application software	Application software (USB version), ToriemonUSB	

\* Dimension for FGP-0.2 ~ 0.5 is 141mm, FGP-100 is 149mm.

## Dimensions





## **DC POWER SUPPLY**

# **PS-30**

**OPERATING MANUAL**

---

The PS-30 DC Power Supply has been carefully engineered and manufactured under rigid quality standards, and should give you satisfactory and dependable operation for many years.

Before placing the equipment in service, we suggest you read through this operating manual to become acquainted with correct operation.

Should any trouble arise with the unit, please contact your dealer, or the nearest KENWOOD service facility, or the factory service facility.

**NOTE:** There are two versions of the PS-30; a 120/220V line model and a 220/240V line model.

## **AFTER UNPACKING**

Save the boxes and packing in the event your unit needs to be transported for temporary operation at a remote location, maintenance, or service.

# INTRODUCTION

The Model PS-30 is a regulated DC power supply designed to match the KENWOOD TS-120S or TS-180S transceiver and provide reliable fixed-station operation. External output terminals (5 A max.) for operation of additional equipment are also provided.

# CAUTIONS

1. The PS-30 will not operate if the output terminals are shorted.

When the power switch of the PS-30 is turned on, make sure that the transceiver's power switch is OFF; otherwise, an output current of more than 2A will flow into the transceiver and signals are transmitted if the transceiver is set in transmit mode.

Turn on the transceiver's power switch after the PS-30 is turned on.

Also, the PS-30 will not operate if the PS-30 power switch is turned on after the transceiver (in transmit mode) is turned on because of the use of a protection circuit.

2. The fuses will blow if the unit is overloaded.
3. Allow sufficient space behind the unit and install in a well-ventilated location.
4. Use the heaviest and shortest DC power cable possible.

If power cable length is excessive, the output voltage will drop or induced RF energy may cause premature protective shutdown of the PS-30.

5. When connecting two or more transceivers to the unit or when using the supply for any other purpose, check that the operating current is below the rated current limit.
6. If the unit is operated without a load, approximately 16 V appears at the output. This is normal and is not an indication of trouble.

# INSTALLATION

Turn the Power Switch OFF before making connections. Connect the AC power cord as shown in Fig. 2. Fig. 3

**Note:** When connecting the unit to the TS-120V (10-W model), use the DC cable supplied with the transceiver.

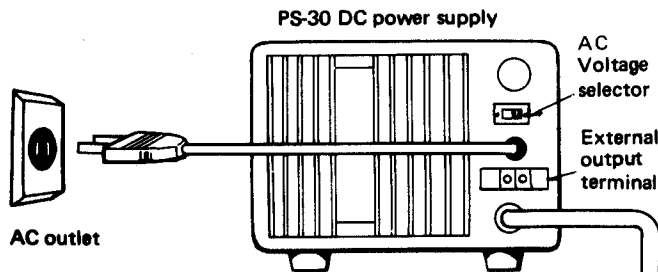


Fig. 2 Connection

# BEFORE USING

The following accessory items are included

Operating manual	..... 1 copy	
Fuse (6A)	..... 1 piece	120/220
Fuse (4A)	..... 1 piece	VAC line model
		220/240
		VAC line model

Extension feet ..... 2 pieces  
Screws, 4mm diameter .... 2 pieces

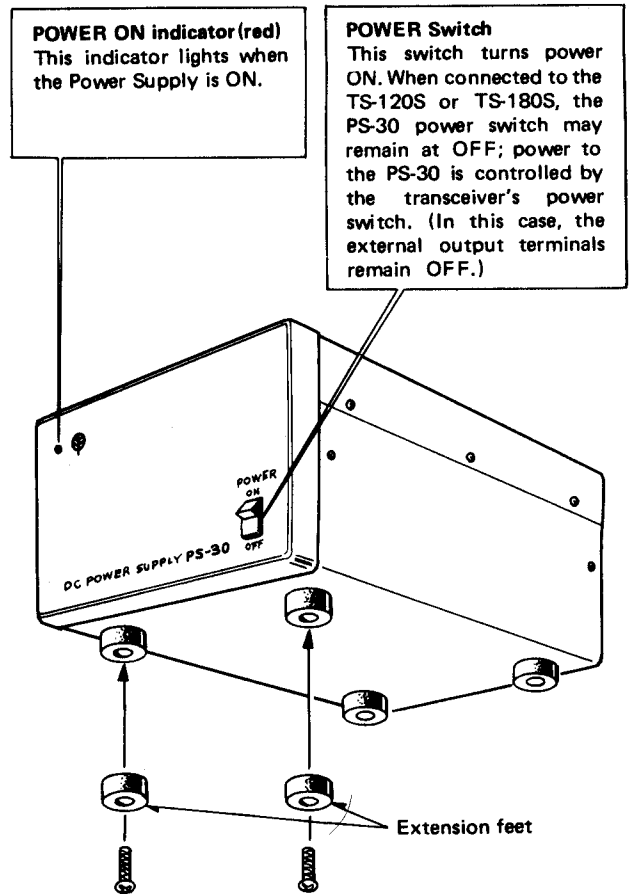
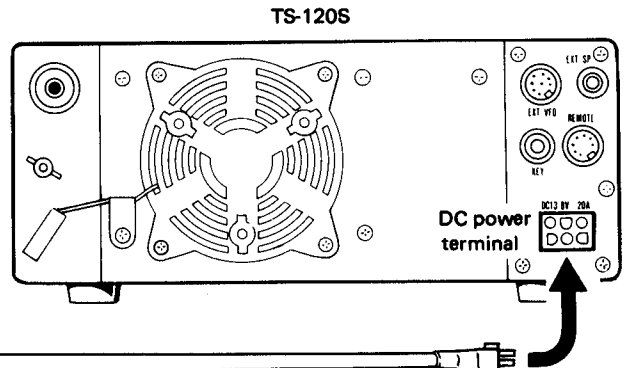
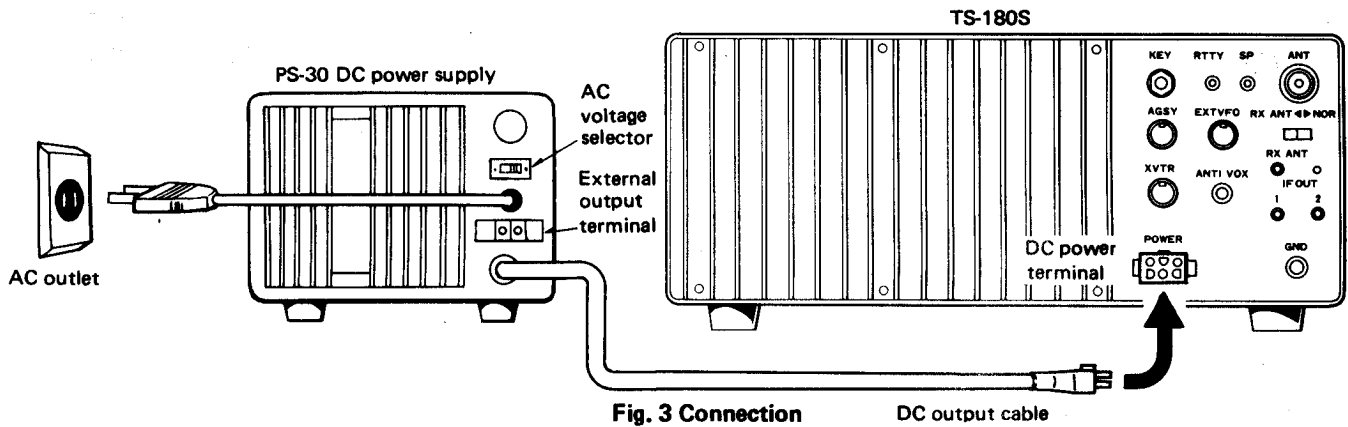


Fig. 1



DC output cable



## MAINTENANCE

1. The supply is equipped with a 6-A or 4-A AC fuse and a 20-A DC fuse. If either one or both blow, DISCONNECT the AC power cable and check for cause before replacing the defective fuse. (Replacement fuses are available from your authorized KENWOOD dealer or service station.)

NEVER use a fuse of higher rating.

2. The unit is designed to deliver 13.8 VDC at 20 A. If, at some future date, the supply should require adjustment, consult your dealer or the nearest KENWOOD service station.

## ADDITIONAL INFORMATION

### 1. GENERAL INFORMATION

Your PS-30 has been factory adjusted and tested to specification before shipment. Under normal circumstances, it will operate in accordance with these operating instructions.

If your power supply fails to work, contact the authorized dealer from which you purchased it for quick, reliable repair.

All adjustments were preset at the factory and should only be readjusted by a qualified technician with proper test equipment.

Attempting service or adjustment without factory authorization can void the power supply's warranty.

### 2. ORDERING SPARE PARTS

When ordering replacement or spare parts for your equipment, be sure to specify the following:

Model and serial number. Schematic number of the part. Printed circuit board number on which the part is located. Part number and name, if known, and Quantity desired.

### 3. SERVICE

Should it ever become necessary to return the equipment for repair, pack in its original box and packing, and include a full, detailed description of the problems involved.

You need not return accessory items unless they are directly related to the service problem.

#### NOTE:

When claiming warranty service, please include a photocopy of the bill of sale, or other proof of purchase showing the date of sale.

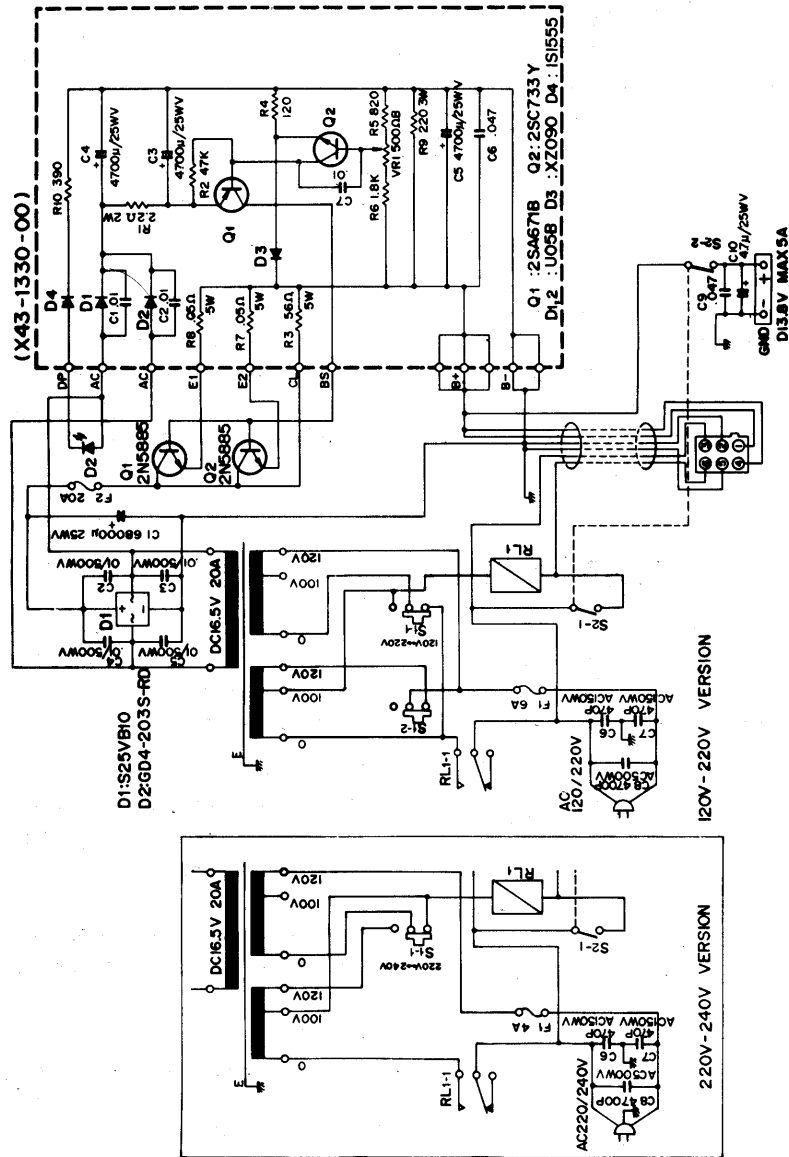
## SPECIFICATIONS

Input voltage:	120/220/240 VAC $\pm$ 10%, 50/60 Hz
Output voltage:	13.8 VDC (standard voltage)
Output current:	20 A (50% duty cycle)
Continuous load current:	15 A max. (including external output terminal)
Output voltage fluctuation:	Within $\pm$ 0.7 V at AC 120V, 220V, 240V $\pm$ 10% (Load current: 15 A) Within 0.7V between 2–15 A load. (No-load output voltage: Less than 16 V at 120/220/240 VAC)
Ripple voltage:	Less than 20 mV (rms) at 13.8 V, output current 15 A.
Power consumption:	Approx. 470 W (at 120/220/240 VAC, 13.8 VDC, 20 A)
Dimensions:	180 (7-1/8)W x 133 (5-1/4)H x 287 (11-5/16)D mm (inch)
Weight:	Approx. 8.9 kg (20 lbs.)

\* Circuit design and ratings are subject to change for improvement without notice.

# SCHEMATIC DIAGRAM

\* Circuit design and ratings are subject to change for improvement without notice.



PS-30

A product of  
**TRIO-KENWOOD CORPORATION**  
 6-17, 3-chome, Aobadai, Meguro-ku, Tokyo 153, Japan

**TRIO-KENWOOD COMMUNICATIONS, INC.**  
 1111, West Walnut Street, Compton, California, 90220, U.S.A  
**TRIO-KENWOOD COMMUNICATIONS, GmbH**  
 D-6374 Steinbach TS, Industriestrasse 8A, West Germany  
**TRIO-KENWOOD (AUSTRALIA) PTY. LTD.**  
 30 Whiting Street, Artarmon, Sydney N.S.W. Australia 2064

By continuing to browse without changing your settings, you accept the use of cookies in order to access services and offers based on your interests in order to improve the user experience on our site. Click on "More info" to find out more about configuring cookies.

[More info \(/cookie-law/\)](#)

I accept

[MENU](#)



## CAPTURE HD PHOTOS & VIDEOS

Amazing footage streamed and recorded directly to your smartphone using the inbuilt 720p HD camera.

## FLY HIGH, FLY SAFE

The cutting edge EPP design of the AR.Drone 2.0 ensures it has a robust structure.

## PILOT LIKE A PRO

With a single touch to your screen, you can control your AR.Drone 2.0 to take-off, land, hover and flip!

I WANT IT (<https://us.store.parrot.com/en/ar-drone-20/296-ar-drone-20-elite-edition.html#/color-sand>)

# Flight Recorder GPS

## Flight Enhancer

Improvement in stabilization

View your flights in 3D

A new control mode: control by map

"Return home" mode

An accessory for developers







## Technical specifications:

Dimensions: 77.7 x 38.3 x 12.5 mm

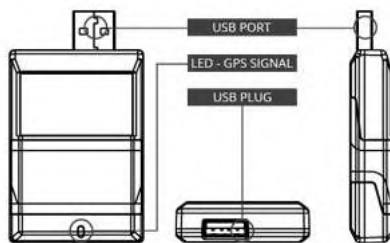
Weight: 31 g

Accuracy: +/- 2 meters

Frequency: 5Hz

Voltage: 5V TBC

Flash memory: 4 GB



LEARN MORE (<https://us.store.parrot.com/en/accessoires-ar-drone-20/223-flight-recorder-3520410011306.html>)

# HD Camera 720p

# *“Live streaming on your smartphone”*

- 720p - 30FPS - H264 encoding base profile
- Low latency streaming
- Video storage on the fly with remote device or with USB flash drive
- JPEG photo capture
- As you fly, the HD video is recorded and sent directly to your device



## WATCH VIDEOS

([https://www.youtube.com/channel/UCF84F\\_NVDIVGkwfPLOWlp7w](https://www.youtube.com/channel/UCF84F_NVDIVGkwfPLOWlp7w))

WATCH PHOTOS (<http://www.parrot.com/usa/gallery/ardrone2/>)

# AR.FreeFlight

*“Impressive, intuitive!”*

AR.FreeFlight is the primary application used to fly and pilot the AR.Drone. Pilot with or without the accelerometer and switch from the frontal camera to the vertical camera.

- Record pictures, nav data & videos and upload them instantly right from the application
- New user friendly interface
- Compatible with AR.Drone and AR.Drone 2.0



**TDOWNLOAD NOW!**



<https://play.google.com/store/apps/details?id=com.parrot.freeflight&hl=en>



<https://itunes.apple.com/en/app/free-flight/id373065271?mt=8>

# Director Mode\*

*“Create high-quality and stable movie shots”*



The Director mode lets you program automatic movements so that you can shoot great videos just like a movie director.

- Choose your movement: traveling, pan, crane...
- Adjust speed and moves in real time to compose your video sequence
- Stabilization system and video post-processing to get clean smooth shots
- Tune camera settings such as white balance, exposure and luminosity
- Selection of key sequences in the video

- Video sharing on YouTube and AR.Drone Academy

\*IN-APP PURCHASE ON AR.FREEFLIGHT

LEARN MORE (<https://www.youtube.com/watch?v=NDcLTcXBr30>)

# Controlling devices



Nvidia Shield console



Epson Moverio display



Thalmic Myo armband



Zeiss Vision Cinemizer OLED glasses



Microsoft surface 2

LEARN MORE (<http://blog.parrot.com/2014/01/06/parrot-ar-drone-2-0-even-more-piloting-possibilities/>)

# AR.Drone Academy

*"Flying in the cloud"*

Live data from registered users

Users



1 291 583

Flights



5 016 805

Hotspots



5 976

Total Flight Time



17Y 19D 16H 0M 44S

Max Speed



11.11m/s

Get more out of your AR.Drone with the AR.Drone Academy. Keep track of all your flights on the Academy map, watch your best videos with added statistical feedback and directly share online with pilots from all over the world!

# Technical Specifications

*“State of the art technology”*



## HD VIDEO RECORDING

Get high definition live video streaming to your smartphone or tablet as you are flying. See a clean, sharp image just as if you were in the pilot seat.

- HD Camera. 720p 30FPS
- Wide angle lens : 92° diagonal
- H264 encoding base profile
- Low latency streaming
- Video storage on the fly with the remote device
- Fotos im JPEG-Format
- Video storage on the fly with Wi-Fi directly on your remote device or on a USB key



## ROBUST STRUCTURE

La structure de l'AR.Drone 2.0 a été conçue pour résister aux figures les plus acrobatiques.

- Carbon fiber tubes : Total weight 380g with outdoor hull, 420g with indoor hull
- High grade 30% fiber charged nylon plastic parts
- Foam to isolate the inertial center from the engines' vibration
- EPP hull injected by a sintered metal mold
- Feuchtigkeitsabweisende Nanobeschichtung auf Ultraschallsensoren
- Fully repairable: All parts and instructions for repairing available on the internet



## ELECTRONIC ASSISTANCE

AR.Drone 2.0 on-board technology gives you extreme precision control and automatic stabilization features.

- 1GHz 32 bit ARM Cortex A8 processor with 800MHz video DSP TMS320DMC64x
- Linux 2.6.32
- 1GB DDR2 RAM at 200MHz
- USB 2.0 high speed for extensions
- Wi-Fi b g n
- 3 axis gyroscope 2000°/second precision
- 3 axis accelerometer +/-50mg precision
- 3 axis magnetometer 6° precision
- Pressure sensor +/- 10 Pa precision
- Ultrasound sensors for ground altitude measurement
- 60 FPS vertical QVGA camera for ground speed measurement



## MOTORS

Fly high. Fly fast. Far away from the ground

- 4 brushless inrunner motors. 14.5W 28,500 RPM
- 1 Micro ball bearing
- 1 Low noise Nylatron gears for 1/8.75 propeller reductor
- 1 Tempered steel propeller shaft
- 1 Self-lubricating bronze bearing
- 1 Specific high propelled drag for great maneuverability
- 1 8 MIPS AVR CPU per motor controller
- Emergency stop controlled by software
- Fully reprogrammable motor controller
- Water resistant motor's electronic controller





## What's in the pack

- 1 AR.Drone 2.0
- 1 Outdoor hull
- 1 Indoor hull
- 1 Charger
- 1 Battery 1000 mAh

## Available colors



Neige



Jungle



Sable

AR.Drone 2.0  
Elite Edition



## What's in the pack

- 1 AR.Drone 2.0
- 1 Outdoor-Rumpf
- 1 Indoor-Rumpf
- 1 Ladegerät
- 2 HD Batterien 1500 mAh
- 3 Sets mit farbigen Propellern

## Available colors



Bleu    Orange    Rouge

AR.Drone 2.0  
Power Edition

BUY AT PARROT (<http://store.parrot.com/fr/ar-drone-20/387-ardrone-20-power-edition-3520410014635.html>)



## What's in the pack

- 1 AR.Drone 2.0
- 1 Outdoor-Rumpf
- 1 Indoor-Rumpf
- 1 Ladegerät
- 1 Batterie 1000 mAh

## Available colors



Bleu



Yellow



Green

# AR.Drone 2.0 Classic

## Accessories



Spare parts

<https://store.parrot.com/en/113-accessoires-ar-drone-20>



Charger

<https://store.parrot.com/fr/accessoires-ar-drone-20/4-chargeur-batterie-ar-drone-20-3520410007330.html>



HD Battery

<https://store.parrot.com/en/113-accessoires-ar-drone-20>



Flight Recorder

<https://store.parrot.com/en/accessoires-ar-drone-20/25-flight-recorder-3520410011306.html>

SPARE PARTS (<https://store.parrot.com/en/113-accessoires-ar-drone-20>)

Join the Parrot AR.Drone community on



<https://www.youtube.com/user/ARdrone>

More information about  
**Ar.Drone 2.0**

email address

>

**Developers**

**Repair**

## Tutorial videos

**Sensefly**

(<https://www.youtube.com/playlist?list=PL1D8828D753A70D9F>)

(<http://www.sensefly.com>)

Parrot designs, develops and markets consumer products for smartphones and tablets as well as high technology solutions in Automotive and UAV business.

[All about parrot \(http://www.parrot.com/usa/aboutparrot\)](http://www.parrot.com/usa/aboutparrot)

About Parrot

[Live now \(http://blog.parrot.com/category/parrot-usa/\)](http://blog.parrot.com/category/parrot-usa/)

[Jobs \(http://recrute.parrot.com/en/offres.php\)](http://recrute.parrot.com/en/offres.php)

[Investor Relations \(http://www.parrot.com/usa/aboutparrot/investorrelations\)](http://www.parrot.com/usa/aboutparrot/investorrelations)

[Automotive \(http://www.parrotoem.com\)](http://www.parrotoem.com)

[Consumer Drones \(http://www.parrot.com/usa/drones/\)](http://www.parrot.com/usa/drones/)

[Professional Drones \(http://www.parrot.com/usa/companies/sequoia/\)](http://www.parrot.com/usa/companies/sequoia/)

Retail Partners

[Certified Installers \(http://certified.parrot.com/index.php\)](http://certified.parrot.com/index.php)

[Find a certified Parrot Car installer in your area \(http://www.parrot.com/usa/cip\)](http://www.parrot.com/usa/cip)

[Parrot Online Store \(https://us.store.parrot.com\)](https://us.store.parrot.com)

Downloads

[Compatibility \(http://www.parrot.com/usa/compatibility\)](http://www.parrot.com/usa/compatibility)

[Apps \(http://www.parrot.com/usa/apps/\)](http://www.parrot.com/usa/apps/)

[Datasheets \(http://www.parrot.com/usa/pdf/\)](http://www.parrot.com/usa/pdf/)



**APPENDIX B:  
EXTRACTED DATA**



rotor speed	Force	volt	current	wat	L/L · E · E	L/W	W/L	CL
1492.23147	101.5536	12.09467	0.78574	5.352824	1	18.97197	0.052709	0.021063
2019.61283	188.65	12.09451	1.339063	11.43527	1.85764	16.4972	0.060616	0.021361
2498.41084	302.3439	12.09486	2.157868	20.56574	2.977186	14.70134	0.068021	0.02237
3012.56136	452.6447	12.09491	3.412203	34.94964	4.4572	12.95134	0.077212	0.023035
3282.67907	542.1878	12.09518	4.221392	44.27924	5.338933	12.24474	0.081668	0.023238
3491.37841	631.1225	12.09524	5.109777	54.6344	6.214673	11.55174	0.086567	0.023912
4017.52075	842.2638	12.09456	7.529795	83.05258	8.293785	10.14133	0.098606	0.024101
4501.76907	1082.619	12.095	10.98216	123.7751	10.66056	8.746661	0.114329	0.024672
4984.86808	1355.048	12.09333	16.40979	188.2726	13.34318	7.197265	0.138942	0.025185
5188.83383	1468.759	12.09444	19.90002	230.1517	14.46289	6.3817	0.156698	0.025195

PROPELLER BLADE PROFILE EXPERIMENT: TYPE 1

rotor speed	Force	volt	current	wat	L/L · E · E	L/W	W/L	CL
1497.46586	71.75355	12.07931	0.644475	3.633031	1	19.75033	0.050632	0.01854
1998.41174	132.1811	12.07911	1.020379	7.564121	1.842154	17.47475	0.057225	0.019177
2496.97612	216.1784	12.07933	1.599507	13.78602	3.01279	15.68098	0.063772	0.02009
2996.50367	320.8121	12.07956	2.401069	22.68178	4.471028	14.14405	0.070701	0.020702
3277.6261	391.7597	12.07911	2.976528	29.17394	5.459796	13.42841	0.074469	0.02113
3492.54793	463.1588	12.07911	3.520719	35.35596	6.454855	13.09988	0.076337	0.022001
4008.88227	619.1629	12.07874	4.975338	52.07314	8.629021	11.89025	0.084102	0.022323
4505.30485	795.421	12.07877	6.90398	74.33658	11.08546	10.70026	0.093456	0.022706
5000.82494	988.0625	12.07813	9.4049	103.4143	13.77023	9.554412	0.104664	0.022892
5489.95892	1203.029	12.0778	12.88055	144.5097	16.76613	8.324907	0.120121	0.023127
5978.15065	1441.101	12.07775	18.27373	208.51	20.08403	6.911423	0.144688	0.023364

PROPELLER BLADE PROFILE EXPERIMENT: TYPE 2

rotor speed	Force	volt	current	wat	L/L · E · E	L/W	W/L	CL
1498.31281	75.85146	12.08575	0.757337	5.001827	1	15.16475	0.065942	0.040595
2013.68464	145.0992	12.08536	1.317599	11.16422	1.912939	12.9968	0.076942	0.042993
2504.78801	232.7577	12.08499	2.127622	20.17959	3.068599	11.53431	0.086698	0.044573
3014.78782	341.826	12.08463	3.271475	33.21318	4.506519	10.29188	0.097164	0.045186
3279.70136	410.9617	12.0844	4.084553	42.58092	5.417981	9.651312	0.103613	0.045904
3514.68975	472.8661	12.08403	4.863092	51.59622	6.234108	9.164744	0.109114	0.045992
4009.51434	626.8289	12.08308	6.952786	75.99203	8.263901	8.248614	0.121232	0.046847
4528.17448	796.8366	12.08305	9.861975	110.1101	10.50523	7.236726	0.138184	0.046691
5018.90267	990.5213	12.08318	13.89937	157.7697	13.0587	6.278273	0.159279	0.047245

PROPELLER BLADE PROFILE EXPERIMENT: TYPE 3

rotor speed	Force	volt	current	wat	L/L · E · E	L/W	W/L	CL
1499.330819	111.0286	12.08325	1.053684	8.581293	1	12.93845	0.077289	0.059341
2021.44531	142.2329	12.0827	1.300358	10.95254	1.281047	12.98629	0.077004	0.041821
2481.184215	230.4309	12.08308	2.122526	20.11269	2.07542	11.45699	0.087283	0.044971
3002.052549	340.2065	12.08306	3.273706	33.2354	3.064134	10.23627	0.097692	0.045354
3286.012278	413.5695	12.08333	4.13368	43.1707	3.724891	9.579865	0.104386	0.046018
3521.845006	476.383	12.08257	4.900807	52.04647	4.290633	9.153032	0.109253	0.046145
4018.399745	621.6516	12.08279	7.003187	76.59835	5.599022	8.11573	0.123217	0.046255
4492.399855	788.099	12.08207	9.903518	110.6031	7.098162	7.125468	0.140342	0.046918
5013.549329	970.9171	12.08215	13.89616	157.7188	8.744748	6.156003	0.162443	0.046409

TIP-INTERVAL EXPERIMENT  $TI/R = 0.03$

rotor speed	Force	volt	current	wat	L/L · E · E	L/W	W/L	CL
1498.31281	75.85146	12.08575	0.757337	5.001827	1	15.16475	0.065942	0.040595
2013.68464	145.0992	12.08536	1.317599	11.16422	1.912939	12.9968	0.076942	0.042993
2504.78801	232.7577	12.08499	2.127622	20.17959	3.068599	11.53431	0.086698	0.044573
3014.78782	341.826	12.08463	3.271475	33.21318	4.506519	10.29188	0.097164	0.045186
3279.70136	410.9617	12.0844	4.084553	42.58092	5.417981	9.651312	0.103613	0.045904
3514.68975	472.8661	12.08403	4.863092	51.59622	6.234108	9.164744	0.109114	0.045992
4009.51434	626.8289	12.08308	6.952786	75.99203	8.263901	8.248614	0.121232	0.046847
4528.17448	796.8366	12.08305	9.861975	110.1101	10.50523	7.236726	0.138184	0.046691
5018.90267	990.5213	12.08318	13.89937	157.7697	13.0587	6.278273	0.159279	0.047245

TIP-INTERVAL EXPERIMENT  $T/R = 0.5$

rotor speed	Force	volt	current	wat	L/L · E · E	L/W	W/L	CL
1495.765646	78.05328	12.086	0.765798	5.001827	1	15.60495	0.064082	0.041916
2009.20349	146.05	12.08573	1.309307	11.16422	1.871157	13.08196	0.076441	0.043468
2504.002298	236.7674	12.08565	2.131536	20.17959	3.033407	11.73301	0.08523	0.04537
3005.126073	349.8205	12.08525	3.304042	33.21318	4.481817	10.53258	0.094943	0.046541
3267.922073	423.5165	12.08538	4.135377	42.58092	5.425992	9.946156	0.100541	0.047648
3526.332867	488.5943	12.08524	4.918935	51.59622	6.259754	9.469576	0.105601	0.047208
3993.142301	640.6257	12.08494	7.032961	75.99203	8.207543	8.430169	0.118622	0.048271
4522.619448	823.7528	12.08544	10.03135	110.1101	10.55373	7.481175	0.133669	0.048387
4995.982754	1019.488	12.08468	14.11683	157.7697	13.06143	6.461871	0.154754	0.049074

TIP-INTERVAL EXPERIMENT  $T/R = 1.0$

## CHAPTER V CONCLUSION

The effect of propeller profile on aerodynamics is investigated by using three types of propellers (i.e. Parrot, enRoute and APC). To sum up the experiment results:

1. The best aerodynamic efficiency in term of hovering condition are both the smaller pitch angle as well as high speed rotation. In this case, propeller Type 3 has the highest lift amongst all. In addition, the best hovering efficiency is achieved by propeller Type 3 also.
2. For the case of rotor-tip interval ( $TI$ ), wider  $TI/R$  corresponds to better hovering efficiency. Both the lift and the hovering efficiency is achieved at the distance of  $TI = 1.0R$ .

This study mainly focused only on the rotor performance (efficiency) of the micro quad-rotor itself. However, other part (i.e. coding) of the program which was utilized to produce simplified data was not explained in very detail manner. It would be very useful if the coding process is included in the explanation.

*This page intentionally left blank*



## REFERENCES

- P. J. Bristeau, F. Callou, D. Vissière, N. Petit, 2011, “The Navigation and Control Technology inside the AR.Drone Micro UAV”, Proceedings of 18th IFAC World Congress, Milano, Italy, pp. 1477–1484.
- Daiki Tsuji, Yuya Yokoama, Yuta Chono, et al., 2014, “Effects of the rotor blade interval on the flow field around a quad-rotor in hovering”, Asia-Pacific International Symposium on Aerospace Technology, APISAT 2014.
- W. Tobo, S. Kataoka, D. Tsuji, M. Munekata, H. Yoshikawa, 2015, “Effects of Side-Walls on the Aerodynamic Characteristics of a Micro Quad-rotor in Hovering”, The 13<sup>th</sup> Asian International Conference on Fluid Machinery, 7<sup>th</sup>-10<sup>th</sup> September 2015, Tokyo, Japan.
- S. Mitsuzaki, D. Tsuji, S. Miyauchi, M. Munekata, H. Yoshikawa, 2015, “The Effect of Rotor-tip Interval and Propeller Profile on the Efficiency of Micro Quad-rotor in Hovering”, 53<sup>rd</sup> Aircraft Symposium, 2015.
- S. A. Raza and W. Gueaieb, 2010, Intelligent Flight Control of Autonomous Quadrotor Federico Casolo (Ed.), ISBN: 978-953-7619-55-8, InTech, Available from: <http://www.intechopen.com/books/motion-control/intelligent-flight-control-of-an-autonomous-quadrotor>. University of Ottawa, Canada.

Sudiyanto, Tata, Mulhowidodo, Agus Budiyo, 2009, First Principle Approach to Modelling of Primitive Quad Rotor. November 2009. International Journal of Aeronautical and Space Sciences Vol 10 No. 2. pp. 148-160.

M. Ragheb. Aerodynamics of Rotor Blades. 2013.

Yanguo, Song, Wang Huanjin, 2009, Design of Flight Control System for a Small Unmanned Tilt Rotor Aircraft. 25 March 2009. Chinese Journal of Aeronautics 22 (2009) pp. 250-256.

Bohorquez, Felipe. Rotor Hover Performance and System Design of an Efficient Coaxial Rotary Wing Micro Air Vehicle. Thesis. University of Maryland, College Park, 2007. Digital Repository at the University of Maryland. Web. Aug. 2010.

## **AUTHOR'S BIOGRAPHY**



Author was born in Surabaya on April 22<sup>nd</sup>, 1994. He is a son of parents Irene Tedjosukmono and Albert Suhud. Prior to entrance of the university, author finished his TK Kristen Petra 9 Surabaya, SDK Petra 9 Surabaya, SMPK Petra 5 Surabaya and SMAK Petra 5 Surabaya. In 2012, author was admitted as student at Department of Marine Engineering, Faculty of Marine Technology, ITS. During his study, author was delegated to Kumamoto University, Japan as an exchange student for one semester. Author was a member of RAMS Laboratory. Author did his intern in PT. JMI, Semarang and PT. Van Oord Indonesia, Batam. Department of Marine Engineering was an unforgettable place for author where he improved his both knowledge and character for better future.

Georgius Suhud

Student of Department of Marine Engineering – Faculty of  
Marine Technology – ITS Surabaya

*georgius@live.com*

*This page intentionally left blank*